Toward Understanding of Toxic Side Effects of a Polyene Antibiotic Amphotericin B: Fluorescence Spectroscopy Reveals Widespread Formation of the Specific Supramolecular Structures…

ARTICLE *in* MOLECULAR PHARMACEUTICS · APRIL 2012

Impact Factor: 4.38 · DOI: 10.1021/mp300143n · Source: PubMed

6 AUTHORS, INCLUDING:

Piotr Wasko
Maria Curie-Sklodowska University in Lublin
5 PUBLICATIONS **17** CITATIONS
SEE PROFILE

Krzysztof Tutaj
University of Rzeszów, Faculty of Biology and …
9 PUBLICATIONS **23** CITATIONS
SEE PROFILE

Wojciech Grudziński
Maria Curie-Sklodowska University in Lublin
39 PUBLICATIONS **667** CITATIONS
SEE PROFILE

Wieslaw I Gruszecki
Maria Curie-Sklodowska University in Lublin
65 PUBLICATIONS **1,312** CITATIONS
SEE PROFILE

molecular pharmaceutics

Article

pubs.acs.org/molecularpharmaceutics

Toward Understanding of Toxic Side Effects of a Polyene Antibiotic Amphotericin B: Fluorescence Spectroscopy Reveals Widespread Formation of the Specific Supramolecular Structures of the Drug

Piotr Wasko, Rafal Luchowski, Krzysztof Tutaj, Wojciech Grudzinski, Przemyslaw Adamkiewicz, and Wieslaw I. Gruszecki*

Department of Biophysics, Institute of Physics, Maria Curie-Skłodowska University, 20-031 Lublin, Poland

Supporting Information

ABSTRACT: Amphotericin B (AmB) is a lifesaving polyene antibiotic used widely to treat deep-seated mycoses. Both the pharmaceutical effectiveness as well as toxic side effects depend on molecular organization of the drug. In the present study, we analyzed steady-state fluorescence, fluorescence anisotropy spectra, fluorescence lifetimes, and fluorescence anisotropy decays of AmB in the systems believed to ensure monomeric organization of the drug and in model lipid membranes. The results of the analyses show that in all of the systems studied, the drug appears in, at least, two spectral forms, interpreted as monomeric and aggregated. Spectroscopic and fluorescence lifetime characteristics of both forms are provided. Interpretation of the fluorescence anisotropy spectra of AmB incorporated into liposomes formed with dipalmitoylphosphatidylcholine let us conclude that monomers of the drug are more tightly bound to the lipid membranes as compared to the aggregates and that AmB aggregates destabilize the membrane structure. Structural model analysis, compared to the analysis of spectral shifts, leads to the conclusion that basic constituents of AmB aggregated structure is a tetramer composed of two hydrogen-bond-stabilized dimers, each dimer formed by molecules twisted by ca. 170°. The tetramer itself can span lipid bilayers and can act as a transmembrane ion channel. Specific aggregate formation of AmB has been concluded as a universal and ubiquitous form of molecular organization of the drug. This process is discussed in terms of toxic side effects of AmB.

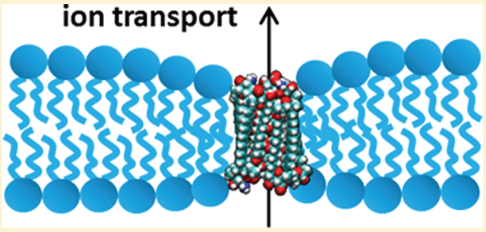

KEYWORDS: *polyene antibiotics, amphotericin B, molecular aggregates, fluorescence anisotropy, biomembranes, antifungal drugs*

INTRODUCTION

Amphotericin B (AmB, Figure 1) is a polyene antibiotic used to treat life-threatening systemic fungal infections.[1] The drug is known and frequently used in a medical practice for more than half of a century owing to its effectiveness and despite of severe and potentially lethal side effects.[2] Despite of the long history of medical applications and research on AmB, the exact molecular mechanism responsible for both mode of therapeutic action and toxic side effects are not fully understood. According to a general conviction, AmB forms transmembrane ion channels that can potentially affect physiological ion transport.[3] The fact that such channels can bind ergosterol, the sterol present in biomembranes of fungi, is a paradigm of selectivity of the drug.[4] However, AmB ion channel formation has been reported also in the lipid systems containing cholesterol[5,6] or even without any sterols.[6,7] Interestingly, the membrane permeability study shows that AmB present in the lipid phase facilitates ion transfer, indeed, but the opposite effect has been reported while AmB was incorporated into the lipid membranes at low concentrations (below 1 mol %). In such a case, the presence of AmB was shown to increase the barrier for the transmembrane proton transfer.[8] The ionophore activity of AmB has been assigned to aggregated, pore-like structures, while the membrane-sealing activity has been assigned to separate molecules of the drug, bound to lipids in the headgroup region. The linear dichroism analysis of AmB in the lipid membrane systems has shown that AmB may be distributed between two pools, one oriented horizontally and one vertically with respect to the membrane plane.[9] Very recently it has been shown that both pools can selectively bind ergosterol[10,11] and sequestration of this membrane-stabilizing agent has been concluded to be primarily responsible for antifungal activity of the drug.[11] Specific molecular interactions of AmB and ergosterol emerged from the results of numerous spectroscopic and structural studies.[12−18] An important problem related to the pharmaceutical activity and applicability of AmB is associated with severe side effects. According to a general understanding, molecular organization forms of AmB, responsible for antifungal activity are also a source of toxicity for patients.[19] Aggregated forms of AmB can be easily detected by means of conventional absorption spectroscopy in the UV−vis region.[20−22] However, the overlap of the spectra of aggregated AmB and vibrational progression spectra of AmB in a

Received: March 13, 2012
Revised: April 12, 2012
Accepted: April 16, 2012
Published: April 16, 2012

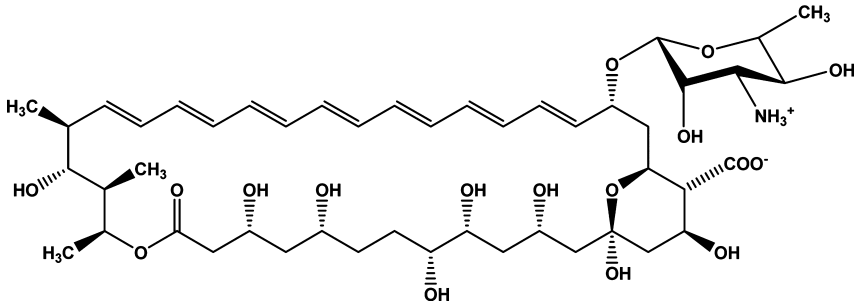

Figure 1. Chemical structure of amphotericin B molecule.

monomeric form makes it difficult to detect molecular organization forms of the drug while present at moderate concentrations. In the present work, we apply the steady-state and time-resolved fluorescence spectroscopy techniques, which appear particularly sensitive to detect and distinguish molecular organization forms of the drug. Our results show that, in all the systems examined, even those believed to ensure monomeric organization of AmB, the drug forms the specific molecular aggregates, which can be responsible for ionophore activity and for destabilization of biomembranes, leading to cell death and for the toxic side effects.

EXPERIMENTAL SECTION

Materials. Crystalline amphotericin B (AmB) and dipalmitoylphosphatidylcholine (DPPC) were purchased from Sigma-Aldrich Chem. Co. (USA). AmB was dissolved in 40% 2-propanol in H_2O and centrifuged for 15 min at 15 000*g* in order to remove microcrystals of the drug still remaining in the sample and was purified by means of HPLC with application of the Supelco Suplex HPLC column (length 25 cm, internal diameter 4.6 mm), with 2-propanol−water mixture (4:6, v:v) as a mobile phase, as described previously.[23−25] Water used for experiments was ultrapure grade, purified with a Milli-Q system from Millipore (France). Specific resistivity was 18.2 MΩ cm. All other chemicals (analytical grade) were obtained from standard vendors.

Sample Preparation. Purified AmB was dried under the stream of gaseous argon and dissolved in water alkalized to a level of pH 12.0, in order to ensure monomeric organization of the drug.[25] The solution was centrifugated for 15 min at 15 000*g* in order to remove aggregated forms of AmB, which may possibly remain in samples. For spectroscopic measurements, samples were diluted to a level of 1.5×10^{-6} M in order to reach the optical density not exceeding the level of 0.2 at the absorption maximum.

In order to prepare AmB-containing liposomes, DPPC was dissolved in chloroform and admixed with pure AmB dissolved in 2-propanol−water (4:6, v/v). Solution was dried under the stream of gaseous argon and then incubated under vacuum for 30 min in order to remove traces of organic solvents. Liposomes were formed in 20 mM Tricine buffer solution (pH 7.6) containing 10 mM KCl. The samples were vortexed at 45 °C (above the main phase transition of DPPC membranes) in order to obtain homogeneous dispersion of large multilamellar vesicles and then sonicated 3 × 5 s with a 20 kHz sonicator with a titanium probe.

Spectroscopic Measurements. Absorption spectra were recorded with Cary 50 UV−vis spectrophotometer (Varian, Australia). Fluorescence spectra were recorded with Cary Eclipse fluorescence spectrophotometer (Varian, Australia). Spectra analysis was performed with application of the Grams/AI software from ThermoGalactic (USA).

Fluorescence lifetime spectra were recoded with FluoTime 300 spectrometer (PicoQuant, Germany). Excitation was at 402.4 nm with 20 MHz frequency of pulses from solid state laser LDH-P-C-405, with pulse width 70 ps (PicoQuant, Germany), and detection performed with multichannel plate and time-correlated single photon counting system PicoHarp 300 (PicoQuant, Germany). Time-decay analyses were performed with the FluoFit Pro v 4.5.3.0 software (PicoQuant, Germany). Fluorescence intensity decays were analyzed by reconvolution with the instrument response function and analyzed as a sum of experimental terms. The data for each experiment were fitted with the following multiexponential model:[26]

$$I(t) = \sum_i \alpha_i \exp(-t/\tau_i) \tag{1}$$

where τ_i are the decay times, and α_i are the pre-exponential factors (amplitudes) of the individual components ($\Sigma\alpha_i = 1$).

Steady-state fluorescence and fluorescence anisotropy spectra were recorded with 390 nm excitation, with application of the long-pass 400 nm emission filter placed in front of the detector, in order to eliminate scattered light. The excitation and emission slits were set to bandwidths of 10 and 5 nm, respectively. In order to eliminate possible contribution from the Raman scattering components,[23,27] fluorescence emission spectra of AmB in solution were calculated as a sum of the spectra recorded with excitation wavelength set to 380 nm, 385 nm, 390 nm, and 395 nm. Before averaging, the (Raman scattering) spectrum recorded under identical conditions with pure solvent (without AmB) had been subtracted, in each case, from the AmB fluorescence emission spectra.

Fluorescence anisotropy spectra were calculated according to the formula

$$r(\lambda) = \frac{VV(\lambda) - GVH(\lambda)}{VV(\lambda) + 2GVH(\lambda)} \tag{2}$$

where VV represents the emission spectra recorded with both the polarizers, placed on the excitation and emission beams, were parallel to each other and perpendicular to the plane of incidence, and VH represents the emission spectra in which the polarizer placed on the excitation beam was perpendicular to the plane of incidence and the emission polarizer was oriented within this plane. G stands for the instrument and wavelength correction factor to compensate for the polarization bias of the detection system.

In the case of the time-resolved measurements, fluorescence anisotropy was calculated according to the formula

$$r(\lambda) = \frac{VV(t) - GVH(t)}{VV(t) + 2GVH(t)} \quad (3)$$

In the latter case, VV and VH correspond to the fluorescence signal at a single excitation and emission wavelength pair. The fluorescence anisotropy decay kinetics provides information on a rotational diffusion correlation time τ_r[26]

$$I(t) = r_0 \exp(-t/\tau_r) \quad (4)$$

where r_o represents the initial (or fundamental) anisotropy. The dependence 4 is strictly valid for spherical particles but can be also applied to provide information on rotational freedom of fluorescing molecules. In the case of isotropic solution, r_o is determined by the angle γ between the direction of the transition dipole moment of the excitation and emission electronic transitions

$$r_0 = (3\cos^2\gamma - 1)/5 \quad (5)$$

All fluorescence measurements have been performed in the right angle configuration of the excitation and observation directions. All kinds of spectroscopic measurements have been repeated at least five times, and the effects presented were found to be highly reproducible.

Molecular Modeling. Molecular interactions between AmB molecules were analyzed and visualized with VMD software support (http://www.ks.uiuc.edu/).[28] VMD has been developed, with NIH support, by the Theoretical and Computational Biophysics group at the Beckman Institute, University of Illinois at Urbana−Champaign. Atomic coordinates of the AmB molecule were used according to the crystallographic structure published recently.[29]

RESULTS

Figure 2 presents the absorption spectrum of AmB recorded in a water−2-propanol solvent mixture (6:4, v/v), reported to ensure monomeric organization of the drug, as in the case of the water solution alkalized to pH 12.[21,25,30,31] The absorption band represents the strongly allowed electronic transition from the ground energy state (S_0, 1^1A_g) to the excited S_2 (1^1B_u) state with very distinct vibrational substructure (the 0−0 transition at 409 nm marked with asterisk). The fluorescence emission spectrum, recorded with the excitation in the 0−0 transition region (Figure 2), presents two distinct bands corresponding to the de-excitation of the S_2 and the S_1 (2^1A_g) energy states[31] (see Figure 3 for diagram of the energy levels). Fluorescence emission from both the energy levels is typical for polyenes characterized by the conjugated double bond system $n = 7$.[32−35] Fluorescence lifetime analysis has been performed with the excitation wavelength close to the 0−0 absorption maximum (402.4 nm) and emission detected at selected wavelengths (Figure 4, see also Table 1). The fluorescence decays recorded at different emission wavelengths have been subjected to global analysis. The fluorescence emission at 460 nm, in the spectral region corresponding to the S_2 state, is characterized by a three-exponential decay with a major (95%), very fast component of $\tau_{M2} \leq 10$ ps, (the time resolution limit of the spectrofluorometer), in accordance to previous reports.[31] Fluorescence emission in the spectral region corresponding to the S_1 state has been probed at three wavelengths: at 523 nm, at 605 nm, and at 650 nm. Interestingly, despite expectations, the global analysis revealed a wavelength-dependence of the fluorescence lifetime amplitudes. The 2.0 ns component, which is present in

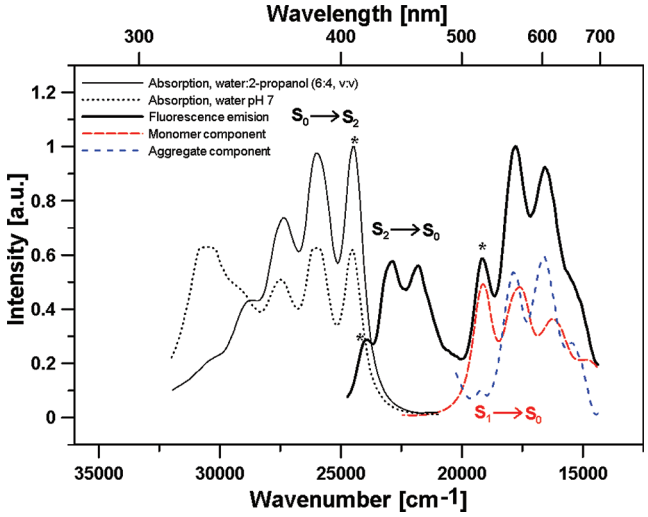

Figure 2. Normalized absorption (1 minus transmission) and fluorescence emission spectra of AmB dissolved in water−2-propanol (6:4, v/v). Fluorescence emission spectrum was obtained as an average of the corrected emission spectra of AmB in solution recorded with excitation at 380, 385, 390, and 395 nm. The emission band in the spectral region below 20 000 cm^{-1} (above 500 nm) is a combination of the fluorescence emission from two states corresponding to different molecular organization forms: monomeric and aggregated (the component spectra obtained by deconvolution are shown). Asterisks mark the spectral origin (0−0 transitions) of the S_2 and S_1 states of the monomeric form. Absorption spectrum of AmB dissolved in water at pH 7.0 is also shown. The AmB concentration in the sample, 1.5×10^{-6} M (please note different extinction coefficient of the aggregated form, ca. 60% of the extinction coefficient of the largely monomeric form, at 409 nm).

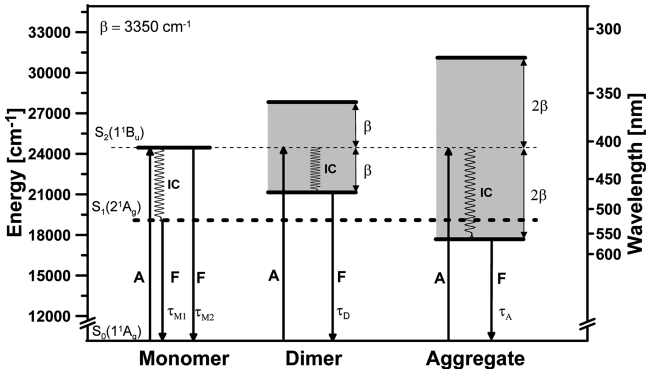

Figure 3. Energy level diagram of AmB in monomeric, dimeric, and aggregated forms based on the absorption and fluorescence emission spectra of AmB. Shaded areas represent excitonic bands. See the text for more explanations.

all the decays recorded in this emission band, can be interpreted as a characteristic lifetime of the $S_1 \rightarrow S_0$ transition of monomeric AmB (τ_{M1}). However, the additional fluorescence decay component, with the lifetime of 350 ps, has been detected, and it is particularly strong at longer wavelengths. This suggests that the emission band, assigned to the $S_1 \rightarrow S_0$ transition is not homogeneous, either due to possible overlap of different electronic energy levels of monomeric AmB or due to the presence of different molecular organization forms in the sample. It is highly probable that the major, short lifetime component of 350 ps represents radiative de-excitation originating from the lowest level (bottom) of the

dx.doi.org/10.1021/mp300143n | Mol. Pharmaceutics 2012, 9, 1511−1520

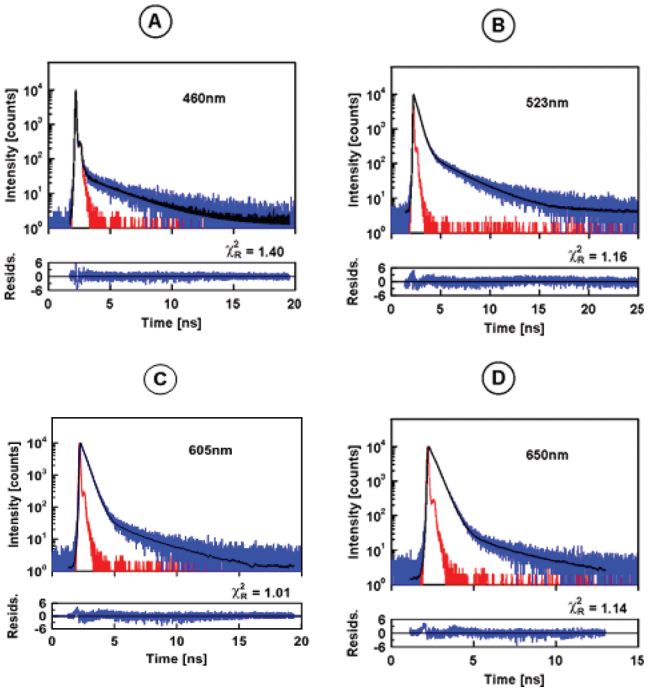

Figure 4. Fluorescence decay kinetics of AmB solution in water alkalized to pH 12 detected at different wavelengths (indicated), presented along with the IRF and residuals of the fit. The multiexponential fit parameters are presented in Table 1.

excitonic band of an aggregated AmB structure, in accordance to the previous report[31] (see Figure 3). It means that, in the case of monomeric fluorophores, emission originates from the S_1 level, while, in the case of the aggregated structures, fluorescence originates from the excitonic band, located below the S_1 level on the energy scale. It is expected that the fluorescence emission yielding from the excitonic band would be higher as compared to the emission from the S_1 state, owing to the fact that the radiative transition $S_1 \rightarrow S_0$ is formally forbidden due to the same symmetry of these two states. The fact that a aggregation-related band is not visible in the long-wavelength region of the absorption spectrum of AmB suggests that the chromophores are oriented roughly parallel to each other and perpendicular to the axis connecting the centers of the transition dipoles of neighboring molecules.[36,37] The light absorption by AmB aggregated structures, in the higher energy region (~30 000 cm^{-1}), can be covered by the absorption spectrum of monomeric AmB, when concentration of the aggregated form is relatively low.[25] Moreover, the effective dipole transition and extinction coefficient is lower in the case of aggregated chromophores.[37] As can be seen from Table 1, an additional, relatively long lifetime component (6.8 ns) has been resolved in result of the global fluorescence decay analysis. Contribution of this component is relatively low, and the fact that its maximum corresponds to the energy gap between the S_2 and S_1 states (490 nm) suggests that this lifetime can correspond to the dimeric structures.[31] This point will be further discussed below.

Figure 5 presents the fluorescence anisotropy spectrum superimposed on a fluorescence emission spectrum of AmB in solution, recorded in the range of the $S_1 \rightarrow S_0$ transition. As can be seen, the anisotropy level recorded is not constant within the range of the emission band. Such a result supports the interpretation according to which the emission band does not originate from a single electronic transition of a single molecular organization form. The fact that the long-wavelength tail of the emission spectrum corresponds to the higher fluorescence anisotropy level, recorded in solution, supports interpretation according to which the long-wavelength-shifted component represents a larger, aggregated form.

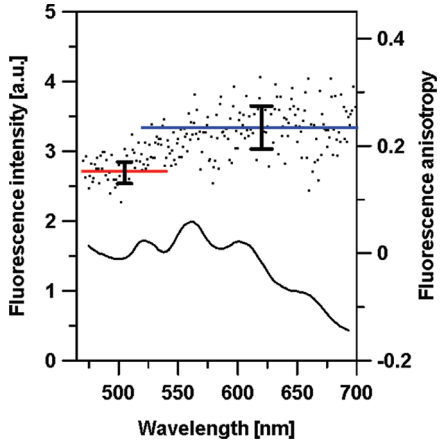

Figure 5. Fluorescence emission (solid line) and fluorescence anisotropy (dots) of AmB in solution (water−isopropanol, 6:4, v/v) excited at 390 nm. Horizontal lines show changes in a fluorescence anisotropy level (calculated as a linear fit to the experimental points) in the spectral range 490−530 nm and 560−700 nm. The standard deviation from the arithmetic mean of the experimental points corresponding to the two linear fits are also presented.

Figure 2 presents an attempt to deconvolute the emission band assigned originally to the $S_1 \rightarrow S_0$ transition. The mirror image of the $S_0 \rightarrow S_2$ absorption band has been copositioned

Table 1. Fluorescence Lifetime Analysis of Amphotericin B Solution in H_2O Alkalized to pH 12 and Incorporated to Liposomes Formed with DPPC

		fraction of a lifetime component (%) at selected emission wavelength				
sample	lifetime component	460 nm	490 nm	523 nm	605 nm	650 nm
pH 12	<10 ps	95	81	14	0	0
	350 ps	0	4	71	96	97
	2.0 ns	2	10	11	4	3
	6.8 ns	3	5	4	0	0
liposomes	<10 ps	92	27	0	0	0
	350 ps	0	10	60	87	90
	2.0 ns	4	36	30	13	10
	6.8 ns	4	27	10	0	0

dx.doi.org/10.1021/mp300143n | *Mol. Pharmaceutics* 2012, 9, 1511−1520

with the 523 nm peak, scaled, and subtracted from the entire fluorescence band recorded. The scaling has been performed arbitrarily, to obtain a component as intensive as possible but not to give a negative component as a result of subtraction from the original fluorescence spectrum.

The shape of the fluorescence emission spectrum of AmB depends on a temperature (Figure 6): the temperature rise

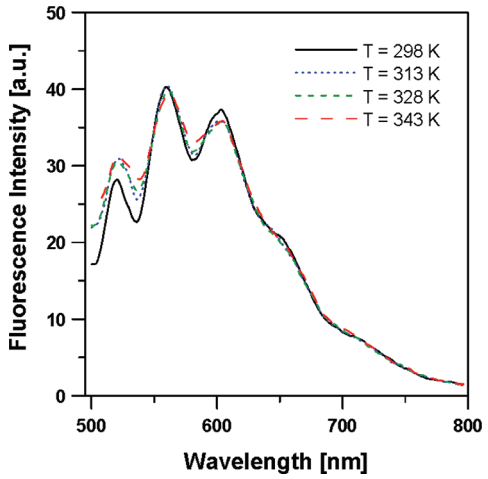

Figure 6. Fluorescence emission spectra of AmB dissolved in water−2-propanol (6:4, v/v) recorded at different indicated temperatures. Excitation at 390 nm.

results in the increase of the 523 nm spectral form and decrease of the spectral form at 605 nm. An assignment of the first band to the monomeric form of AmB and the second band to the aggregated one let analyze the spectral changes observed in terms of the Van't Hoff formalism (Figure 7). The assumption that a structure is composed of 4 chromophores leads to the

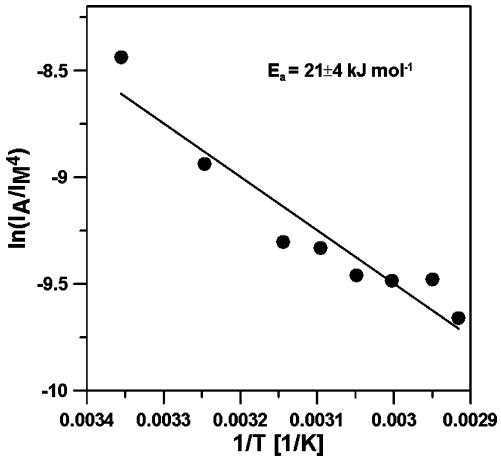

Figure 7. Van't Hoff analysis of the fluorescence emission spectra of AmB dissolved in water−2-propanol (6:4, v/v), recorded at different temperatures, as presented in Figure 1. Spectral intensity corresponding to monomers (I_M) and aggregates (I_A) has been calculated based on the deconvolution as presented in Figure 2. Briefly, $I_M = (0.86I_{523} - 0.39I_{605})/0.47$ and $I_A = (0.62I_{605} - 0.14I_{523})/0.47$. Association energy for a tetrameric structure was calculated according to the equation: $I_A/I_A^N = C \exp(E_a/kT)$, for $N = 4$. Experimental points correspond to the spectra presented in Figure 6. The association energy calculated as arithmetic mean from 5 independent experiments is $E_a = 21 \pm 4$ kJ mol^{-1}.

association energy of 21 ± 4 kJ mol^{-1}. The straightforward interpretation of association energy would be based on a model in which AmB molecules interact to each other via the dipole−dipole interactions between the polyene chains of neighboring molecules in a hydrophilic medium. However, the association energy determined is relatively high and let us conclude that the molecular structure is stabilized by a network of strong or weak hydrogen bonds.[38,39]

Fluorescence anisotropy decay analysis has been performed to analyze further the AmB spectral forms overlapped in the region assigned originally to the $S_1 \rightarrow S_0$ transition (see Figure 8 and Table 2). The decays recorded at different wavelengths were well characterized with the single-exponential processes in the case of the AmB solutions and two-exponential in the case of AmB incorporated to liposomes (Table 2). The rotational diffusion correlation time determined in the AmB solution at 460 nm (0.35 ns) is clearly shorter than the one determined at longer wavelengths, which goes along with our interpretation that light emission in this spectral region can be associated with de-excitation of larger molecular structures than the AmB monomer. Surprisingly, the r_o level corresponding to the putative aggregated structure (0.27 at 650 nm) is lower than in the case of monomeric AmB (0.39 at 460 nm). This effect can be interpreted in terms of energy delocalization over the entire aggregated structure and emission from the chromophore, which is different (twisted) from this one involved in light absorption. In the case of the aggregated structure (probed at 650 nm), the r_o corresponds well to the static fluorescence anisotropy level (Figure 5). In the case of monomeric AmB, fast rotation leads to the static fluorescence anisotropy level (r) lower than r_o for monomers and also lower than the r parameter determined for the aggregated structures. In the case of AmB incorporated to liposomes, the r_o values are very similar to those determined for the drug in the solution (Table 2). However, the fluorescence anisotropy decays of AmB in liposomes are very different from those in solution (see Figure 8) and have to be analyzed in terms of two-exponential processes. In each case (emission wavelength, see Table 2), one component is in the order of magnitude and comparable to the rotational correlation time of AmB in water solution ($^1\tau_r$) and the second, much longer ($^2\tau_r$) has to be attributed to the AmB fraction bound more tightly, presumably to the lipid membranes.

Figure 9 presents the fluorescence anisotropy analyses of AmB in solution and incorporated into model lipid membranes formed with dipalmitoylphosphatidylcholine (DPPC). The analyses have been performed at the fluorescence emission wavelengths characteristic of monomeric and aggregated AmB. The fact that the anisotropy level in solution is higher in the case of the AmB aggregates, as compared to monomers, reflects the fact that monomers possess higher diffusional freedom in the solution. In the case of both molecular organization forms, the fluorescence anisotropy level decreases with the temperature increase (increase in the diffusional freedom). Surprisingly, upon AmB binding to lipid membranes, the fluorescence anisotropy level in the case of monomers is much higher than in the case of the aggregates. Such an effect indicates that AmB monomers are more tightly bound to the lipid membranes as compared to more complex molecular structures. Interestingly, the fluorescence anisotropy of monomeric AmB increases sharply at temperatures corresponding to the phase pretransition of the membranes formed with DPPC ($L_{\beta'} \rightarrow P_{\beta'}$, 35 °C), despite the temperature rise. This anomalous effect represents,

dx.doi.org/10.1021/mp300143n | Mol. Pharmaceutics 2012, 9, 1511−1520

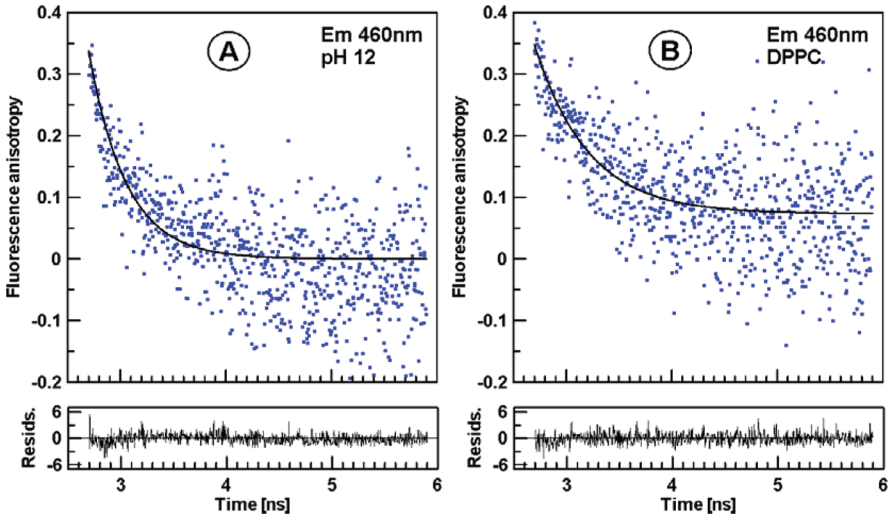

Figure 8. Fluorescence anisotropy decays of AmB in the solution in water alkalized to pH 12 (A) and incorporated to DPPC liposomes at a concentration of 5 mol % with respect to lipid (B). Excitation is at 402.4 nm. Parameters of exponential analysis of the decays are presented in Table 2.

Table 2. Fluorescence Anisotropy Decay Analysis of Amphotericin B Solution in H_2O Alkalized to pH 12 and Incorporated to Liposomes Formed with DPPC

		value of decay parameters at selected emission wavelengths				
sample	decay parameter	460 nm	490 nm	523 nm	605 nm	650 nm
pH 12	r_o	0.39	0.33	0.38	0.34	0.27
	τ_r (ns)	0.35	0.50	0.83	0.72	0.58
liposomes	r_o	0.40	0.28	0.32	0.35	0.30
	$^1\tau_r$ (ns)	0.50 (51%)	0.37 (56%)	0.70 (87%)	0.76 (59%)	0.65 (55%)
	$^2\tau_r$ (ns)	547 (49%)	3.55 (44%)	288 (13%)	2547 (41%)	2753 (45%)

most probably, a mechanism of penetration of the drug molecules deeper into the membrane structure, under conditions of formation of the ripple phase. Such an effect is not visible in the DPPC membrane system modified with 5 mol % AmB. In the latter case, the fluorescence anisotropy level of AmB remains generally at a higher level both in the case of monomeric and aggregated organization forms. This effect can be interpreted in terms of a rigidifying mechanism of the additive with respect to the lipid phase or in terms of formation of aggregated structures of AmB, characterized by relatively restricted diffusional freedom. The fact that fluorescence anisotropy calculated for AmB aggregates in the system containing 1 mol % and 5 mol % of the antibiotic are essentially different, suggests different localization of aggregated structures in those membrane systems studied.

DISCUSSION

In the present work, we examined molecular organization of a polyene antibiotic amphotericin B in the systems believed to ensure monomeric organization of the drug. This problem seems to be particularly important owing to the fact that, despite widespread use of this antibiotic in a medical practice, for more than half of a century, molecular mechanisms responsible for both therapeutic action and severe side effects are not fully understood. Pharmaceutical practice shows that the application of AmB in the form of a detergent dispersion (Fungizone) or a lipid dispersion (Ambisome) can reduce the antibiotic toxicity for patients. Very recently, it has been proposed that binding of ergosterol, a sterol compound present in biomembranes of fungi, can explain amphotericin B selectivity and antifungal activity.[11] The ion-channel-forming activity of AmB has been concluded as a complementary activity that can further increase the drug potency.[11] However, this latter mechanism can be responsible for the toxicity for patients owing to the fact that the channel-forming activity and affection of a transmembrane ion transport can be basically independent of a presence of ergosterol in the membrane system.[6−8] The results of the spectroscopic studies, presented in this work show, without doubt, that molecular aggregation forms of AmB are present in the systems believed to ensure monomeric organization of the drug. One of such a system is a solution of AmB in water alkalized to pH 12.[24,25] AmB is a zwitterion, and at pH values higher than 10, the drug possesses negative electric charge (due to ionized group COO^-), and therefore, formation of molecular assemblies is limited, owing to the electrostatic repulsion.[25] Steady-state fluorescence, fluorescence anisotropy, and fluorescence lifetime analyses, presented above, show that molecular organization forms, which are present, are characterized by a relatively large spectral shift (6700 cm^{-1}). The spectral shift is proportional to the square of the dipole transition moment (μ^2), and therefore, such a pronounced spectral shift has to originate from the strongly allowed electronic transition $S_0 \rightarrow S_2$. Taking into consideration the dipole transition value of AmB (μ = 11.3 D), refractive index of water (η = 1.33), assuming formation of H-type aggregates (κ = 1), and that maximum spectral shift corresponds to 2β (where β is a dipole−dipole coupling matrix element), one can calculate a distance between the neighboring chromophores in the aggregated structure of AmB as 0.48 nm, based on the dependency[9,37]

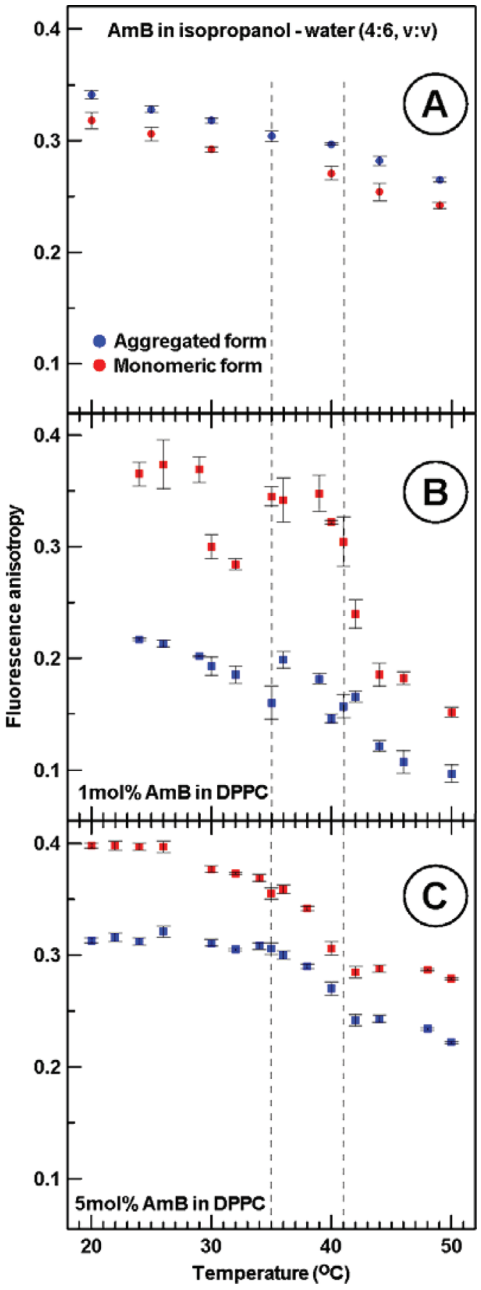

Figure 9. Temperature dependencies of a steady-state fluorescence anisotropy parameter of AmB dissolved in water−2-propanol (6:4, v/v) (A) and incorporated to DPPC liposomes at the concentration of 1 mol % (B) and 5 mol % (C) with respect to lipid. Fluorescence anisotropy was determined for the spectral form corresponding to AmB monomers (the spectral region 490−530 nm) and aggregated structures (560−700 nm) according to the method shown in Figure 5. Experimental points represent arithmetic mean from 3 to 5 experiments ± SD. Dashed lines point the specific temperatures of the phase pretransition and transition for the lipid membranes formed with DPPC.

$$\beta = 5.04\frac{|\mu|^2}{\eta^2 R^3}\kappa \qquad (6)$$

Such a small distance implies relatively tight packing of unpolar polyene chains, which is understandable in the case of the antibiotic dispersion in a water phase. Energy minimization in such a structure requires the electrically charged groups to be separated and located as far as possible. Therefore, it is very likely that neighboring interacting molecules are antiparallel relative to one another. Interestingly, the molecular dynamic studies on a formation of AmB dimers in water show exceptional stability of the structure in which interacting molecules form an angle of about 170°, and the dynamically averaged distance between the centers of the chromophores is equal to 0.49 nm.[40] The chromophore−chromophore distance in the AmB aggregated structure in water, calculated above on the basis of the spectroscopic analysis, 0.48 nm, is exceptionally close to that one found from the molecular dynamics study for the dimeric structure. Because of that, it is very likely that the molecular assembly of the drug, formed in the water phase, is constituted out of the dimeric subunits. A model of such a structure is presented in Figure 10. Relatively high association energy of AmB aggregates, concluded from the van't Hoff analysis (21 ± 4 kJ mol^{-1}, Figure 7), can be explained in terms of AmB dimerization driving forces, which originate from the hydrophobic interactions with significant participation of hydrogen bonds.[40] The dimeric structure of AmB, modeled in Figure 10B, is stabilized via the dipole−dipole interactions between chromophores (center-to-center distance 0.48 nm) and additionally, via two hydrogen bonds, between the hydroxyl groups C(35)−OH and oxygen C(42)−O−C(19), in agreement to the molecular dynamics calculations.[40] Molecular modeling shows that such dimers can easily associate into the tetrameric structures (Figure 10C) in which two AmB dimers are linked via the hydrogen bond network: C(8)−OH···OH-C(3), as depicted in the model. Such a molecular aggregate of AmB adopts a pore-like structure (as can be seen from Figure 10C), and its roughly elliptical cross-section (0.40 × 0.75 nm) enables, in principle, transmembrane proton transport, providing that such a structure can penetrate the lipid bilayer. Transmembrane localization of the tetrameric AmB structure (as proposed in the model presented in Figure 10D) seems to be highly probable for two reasons. The first reason is the fact that the outer surface of this structure is constituted by the hydrophobic polyene chains and may easily accommodate into the hydrophobic membrane core. The second reason is a distance between the polar mycosamine sugar groups located at the opposite ends of the tetrameric structure, 3.2 nm, which corresponds very well to the thickness of the hydrophobic core of lipid membranes. For example, the hydrophobic core of the membranes formed with egg yolk phosphatidylcholine (EYPC) has been determined as 2.26 nm,[41] in the case of dimirystoylphosphatidylcholine (DMPC) as 2.54 nm,[42] in the case of plant thylakoid membranes as 3.0 nm,[43] and in the case of DPPC as 3.22 nm.[41] The hydrophobic outer surface of the tetramers of AmB implies that such structures will assemble into more complex structures, both in the water and membrane environments, via the van der Waals interactions between the long and rigid polyene chains.

Interestingly, the hypsochromically shifted shoulder in the absorption spectra of AmB incorporated to liposomes appears in the region between 330 and 350 nm,[9,22,44] very close to the absorption maximum corresponding to the AmB aggregated structure in the water solution at pH 7.0 (325 nm, see Figure 2).[25,31] This means that, despite very different environments, water versus lipid membrane core, the structures formed by AmB molecules are characterized by very similar distances between the centers of the neighboring chromophores. Incorporation of AmB into the lipid membrane system results in the hypsochromic shift from 408 to 330 nm (2β = 5793

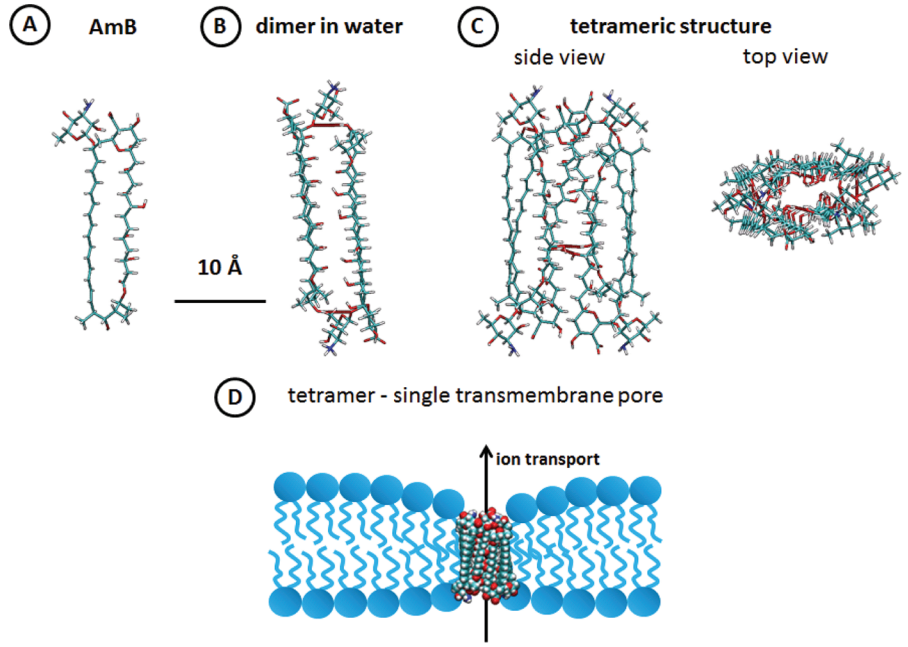

Figure 10. Atomic model of AmB molecule (A), AmB dimer in water based on the molecular dynamics calculation[40] (B), tetrameric structure composed of two dimers and stabilized via hydrogen bonds (C), and a model of incorporation of the tetrameric AmB structure into the lipid bilayer (D). Structural properties and dimensions of the tetrameric structure of AmB enable transmembrane ion transport. Atomic coordinates of AmB are based on the crystallographic structure.[29] Molecular interactions between AmB molecules were analyzed and visualized with VMD software support (http://www.ks.uiuc.edu/). VMD has been developed, with NIH support, by the Theoretical and Computational Biophysics group at the Beckman Institute, University of Illinois at Urbana−Champaign.

cm^{-1}), which corresponds to the distance R = 0.47 nm, as can be calculated according to eq 6, assuming the refractive index of the hydrophobic membrane core as 1.40.[22] Comparison of the chromophore distances in the aggregated structures formed by AmB in water and in the environment of lipid membranes let us conclude that virtually the same type of molecular structures are formed in those two environments, instead of hydrophobic and hydrophilic pores predicted as based on the chemical structure of the drug[7,45] and molecular dynamics analysis.[4] It seems therefore very likely that the aggregated structures formed are constituted of the same dimeric subunits. The expected spectral shift accompanying the dimer formation is β, half of that observed in the case of an aggregated structure composed of a large number of molecules. If present in the sample, the dimeric forms have to be represented by a spectral band in the absorption spectrum, which overlaps with the vibrational substructure of the $S_0 \rightarrow S_2$ transition and a spectral band in the fluorescence emission spectrum between the $S_2 \rightarrow S_0$ and $S_1 \rightarrow S_0$ bands (see Figure 2). The dimeric form of AmB has been assigned to particularly long fluorescence lifetime[31] and is represented in the present analysis by a 6.8 ns component (see Table 1). As can be seen, this component is particularly intensive at 490 nm, in the spectral region between the bands assigned to the $S_2 \rightarrow S_0$ and $S_1 \rightarrow S_0$ transitions. Interestingly, the dimer-assigned fluorescence lifetime components are particularly pronounced in the case of AmB incorporated into the lipid membranes (27% contribution, see Table 1). Dimeric AmB in the lipid membranes has also very distinctive signature in the fluorescence anisotropy decay (see the column corresponding to 490 nm in Table 2). The slow component of the monomeric, membrane-bound AmB is in the order of magnitude of 0.1 μs and in the case of the aggregated structures in the order of magnitude of 1 μs, both typical of diffusional rotation within the lipid membranes or even of whole liposomal structures. As can be seen, the slow component attributed to the dimeric structures (3.55 ns) reflects relatively high motional freedom of AmB dimers within the lipid bilayer. Such a freedom implies efficiency in assembly into more complex molecular structures, including transmembrane tetrameric pores. As discussed above, the AmB dimers are already formed in the water phase and can penetrate into the membranes much more efficient than more complex and more sized molecular structures. As shown in the present study, the experimental systems believed to ensure monomeric organization of AmB contain also dimeric and aggregated structures of the drug, which can be potentially bound to the biomembranes. Such a mechanism can be considered as a potential source of severe side effects of the drug.

CONCLUSIONS

Here, we report that dimers and molecular aggregates of a polyene antibiotic amphotericin B are present in all the examined systems, including those believed to ensure monomeric organization of the drug. Such conclusion is based on the analysis of the steady-state and time-resolved fluorescence and fluorescence anisotropy of amphotericin B (autofluorescence). The fact that both the dimeric and also aggregated structures of amphotericin B are formed even by the drug molecules, which are electrically charged (at pH 12), implies antiparallel orientation of neighboring molecules in the structures examined. Such an organization model is consistent with the AmB organization models based on the molecular dynamics calculations. In such aggregated (tetrameric), pore-like structures, the polar mycosamine headgroups are exposed at two opposite sides. This can be responsible for membrane binding and transmembrane localization of AmB aggregated structures with respect to the lipid bilayers. It is very likely that the presence of dimers and tetrameric molecular aggregates of

AmB is primarily responsible for severe toxic side effects for patients. This conclusion is setting new directions in the search of a pharmacologic formula of the drug with minimized side effects.

■ ASSOCIATED CONTENT

Supporting Information

AmB tetramer structure (presented in Figure 10C) in the mpg format. This material is available free of charge via the Internet at http://pubs.acs.org.

■ AUTHOR INFORMATION

Corresponding Author

*Department of Biophysics, Institute of Physics, Maria Curie Sklodowska University 20-031 Lublin, Poland. Tel: + (48 81) 537 62 52. Fax: + (48 81) 537 61 91. E-mail: wieslaw.gruszecki@umcs.pl.

Notes

The authors declare no competing financial interest.

■ ACKNOWLEDGMENTS

Thanks are due to Professor Mariusz Gagos for providing us with the most recent and accurate crystallographic data and atomic coordinates of amphotericin B. This research has been performed within the framework of the project "Molecular Spectroscopy for BioMedical Studies" financed by the Foundation for Polish Science within the TEAM program.

■ ABBREVIATIONS USED

AmB, amphotericin B; DPPC, dipalmitoylphosphatidylcholine

■ REFERENCES

(1) Baginski, M.; Cybulska, B.; Gruszecki, W. I. Interaction of Macrolide Antibiotics with Lipid Membranes. In *Advances in Planar Lipid Bilayers and Liposomes*; Ottova-Liu, A., Ed.; Elsevier Science Publishers: Amsterdam, The Netherlands, 2006; Vol. 3, pp 269−329.

(2) Mora-Duarte, J.; Betts, R.; Rotstein, C.; Colombo, A. L.; Thompson-Moya, L.; Smietana, J.; Lupinacci, R.; Sable, C.; Kartsonis, N.; Perfect, J. Comparison of caspofungin and amphotericin B for invasive candidiasis. *N. Engl. J. Med.* **2002**, *347*, 2020−2029.

(3) De Kruijff, B.; Gerritsen, W. J.; Oerlemans, A.; Demel, R. A.; van Deenen, L. L. Polyene antibiotic-sterol interactions in membranes of Acholeplasma laidlawii cells and lecithin liposomes. I. Specificity of the membrane permeability changes induced by the polyene antibiotics. *Biochim. Biophys. Acta* **1974**, *339*, 30−43.

(4) Baginski, M.; Resat, H.; McCammon, J. A. Molecular properties of amphotericin B membrane channel: a molecular dynamics simulation. *Mol. Pharmacol.* **1997**, *52*, 560−570.

(5) Yilma, S.; Cannon-Sykora, J.; Samoylov, A.; Lo, T.; Liu, N.; Brinker, C. J.; Neely, W. C.; Vodyanoy, V. Large-conductance cholesterol-amphotericin B channels in reconstituted lipid bilayers. *Biosens. Bioelectron.* **2007**, *22*, 1359−1367.

(6) Cotero, B. V.; Rebolledo-Antunez, S.; Ortega-Blake, I. On the role of sterol in the formation of the amphotericin B channel. *Biochim. Biophys. Acta* **1998**, *1375*, 43−51.

(7) Bonilla-Marin, M.; Moreno-Bello, M.; Ortega-Blake, I. A microscopic electrostatic model for the amphotericin B channel. *Biochim. Biophys. Acta* **1991**, *1061*, 65−77.

(8) Herec, M.; Dziubinska, H.; Trebacz, K.; Morzycki, J. W.; Gruszecki, W. I. An effect of antibiotic amphotericin B on ion transport across model lipid membranes and tonoplast membranes. *Biochem. Pharmacol.* **2005**, *70*, 668−675.

(9) Gruszecki, W. I.; Gagos, M.; Herec, M. Dimers of polyene antibiotic amphotericin B detected by means of fluorescence spectroscopy: molecular organization in solution and in lipid membranes. *J. Photochem. Photobiol., B* **2003**, *69*, 49−57.

(10) Umegawa, Y.; Nakagawa, Y.; Tahara, K.; Tsuchikawa, H.; Matsumori, N.; Oishi, T.; Murata, M. Head-to-tail interaction between amphotericin B and ergosterol occurs in hydrated phospholipid membrane. *Biochemistry* **2012**, *51*, 83−89.

(11) Gray, K. C.; Palacios, D. S.; Dailey, I.; Endo, M. M.; Uno, B. E.; Wilcock, B. C.; Burke, M. D. Amphotericin primarily kills yeast by simply binding ergosterol. *Proc. Natl. Acad. Sci. U.S.A.* **2012**, DOI: 10.1073/pnas.1117280109.

(12) Baginski, M.; Resat, H.; Borowski, E. Comparative molecular dynamics simulations of amphotericin B-cholesterol/ergosterol membrane channels. *Biochim. Biophys. Acta* **2002**, *1567*, 63−78.

(13) Baran, M.; Mazerski, J. Molecular modelling of amphotericin B−ergosterol primary complex in water. *Biophys. Chem.* **2002**, *95*, 125−133.

(14) Barwicz, J.; Tancrede, P. The effect of aggregation state of amphotericin-B on its interactions with cholesterol- or ergosterol-containing phosphatidylcholine monolayers. *Chem. Phys. Lipids* **1997**, *85*, 145−155.

(15) Charbonneau, C.; Fournier, I.; Dufresne, S.; Barwicz, J.; Tancrede, P. The interactions of amphotericin B with various sterols in relation to its possible use in anticancer therapy. *Biophys. Chem.* **2001**, *91*, 125−133.

(16) Gabrielska, J.; Gagos, M.; Gubernator, J.; Gruszecki, W. I. Binding of antibiotic amphotericin B to lipid membranes: a 1H NMR study. *FEBS Lett.* **2006**, *580*, 2677−2685.

(17) Hac-Wydro, K.; Dynarowicz-Latka, P.; Grzybowska, J.; Borowski, E. Interactions of amphotericin B derivative of low toxicity with biological membrane components: the Langmuir monolayer approach. *Biophys. Chem.* **2005**, *116*, 77−88.

(18) Seoane, R.; Minones, J.; Conde, O.; Casas, M.; Iribarnegaray, E. Molecular organisation of amphotericin B at the air−water interface in the presence of sterols: a monolayer study. *Biochim. Biophys. Acta* **1998**, *1375*, 73−83.

(19) Barwicz, J.; Christian, S.; Gruda, I. Effects of the aggregation state of amphotericin B on its toxicity to mice. *Antimicrob. Agents Chemother.* **1992**, *36*, 2310−2315.

(20) Hemenger, R. P.; Kaplan, T.; Gray, L. J. Structure of amphotericin B aggregates based on calculations of optical spectra. *Biopolymers* **1983**, *22*, 911−918.

(21) Barwicz, J.; Gruszecki, W. I.; Gruda, I. Spontaneous organization of amphotericin B in aqueous medium. *J. Colloid Interface Sci.* **1993**, *158*, 71−76.

(22) Gagos, M.; Koper, R.; Gruszecki, W. I. Spectrophotometric analysis of organisation of dipalmitoylphosphatylcholine bilayers containing the polyene antibiotic amphotericin B. *Biochim. Biophys. Acta* **2001**, *1511*, 90−98.

(23) Gagos, M.; Arczewska, M.; Gruszecki, W. I. Raman spectroscopic study of aggregation process of antibiotic amphotericin B induced by H+, Na+, and K+ ions. *J. Phys. Chem. B* **2011**, *115*, 5032−5036.

(24) Gagos, M.; Gabrielska, J.; Dalla Serra, M.; Gruszecki, W. I. Binding of antibiotic amphotericin B to lipid membranes: Monomolecular layer technique and linear dichroism-FTIR studies. *Mol. Membr. Biol.* **2005**, *22*, 433−442.

(25) Gagos, M.; Herec, M.; Arczewska, M.; Czernel, G.; Dalla Serra, M.; Gruszecki, W. I. Anomalously high aggregation level of the polyene antibiotic amphotericin B in acidic medium: implications for the biological action. *Biophys. Chem.* **2008**, *136*, 44−49.

(26) Lakowicz, J. R. *Principles of Fluorescence Spectroscopy*; Springer: New York, 2006.

(27) Bolard, J.; Cheron, M.; Cleary, J. D.; Kramer, R. E. The contribution of Raman scattering to the fluorescence of the polyene antibiotic amphotericin B. *J. Fluoresc.* **2011**, *21*, 831−834.

(28) Humphrey, W.; Dalke, A.; Schulten, K. VMD: Visual molecular dynamics. *J. Mol. Graphics* **1996**, *14*, 33−38.

(29) Jarzembska, K. N.; Kaminski, D.; Hoser, A. A.; Malińska, M.; Senczyna, B.; Woźniak, K.; Gagoś, M. Controlled crystallisation,

structure and molecular properties of iodoacetylamphotericin B. *Cryst. Growth Des.* **2012**, DOI: 10.1021/cg2017227.
(30) Gagos, M.; Gruszecki, W. I. Organization of polyene antibiotic amphotericin B at the argon−water interface. *Biophys. Chem.* **2008**, *137*, 110−115.
(31) Gruszecki, W. I.; Luchowski, R.; Gagos, M.; Arczewska, M.; Sarkar, P.; Herec, M.; Mysliwa-Kurdziel, B.; Strzalka, K.; Gryczynski, I.; Gryczynski, Z. Molecular organization of antifungal antibiotic amphotericin B in lipid monolayers studied by means of fluorescence lifetime imaging microscopy. *Biophys. Chem.* **2009**, *143*, 95−101.
(32) Christensen, R. L. The electronic states of carotenoids. In *The Photochemistry of Carotenoids*; Frank, H. A., Young, A. J., Britton, G., Cogdell, R. J., Eds.; Kluwer Academic Publishers: Dordrecht, The Netherlands, 1999; pp 137−156.
(33) Andersson, P. O.; Bachilo, S. M.; Chen, R.-L.; Gillbro, T. Solvent and temperature effects on dual fluorescence in a series of carotenes. Energy gap dependence of the internal conversion rate. *J. Phys. Chem. A* **1995**, *99*, 16199−16209.
(34) Frank, H. A.; Desamero, R. Z. B.; Chynwat, V.; Gebhard, R.; Van der Hoef, I.; Jansen, F. J.; Lugtenburg, J.; Gosztola, D.; Wasielewski, M. R. Spectroscopic properties of spheroidene analogs having different extents of pi-electron conjugation. *J. Phys. Chem. A* **1997**, *101*, 149−157.
(35) Frank, H. A.; Josue, J. S.; Bautista, J. A.; van der Hoef, I.; Jansen, F. J.; Lugtenburg, J.; Wiederrecht, G.; Christensen, R. L. Spectroscopic and photochemical properties of open-chain carotenoids. *J. Phys. Chem. B* **2002**, *106*, 2083−2092.
(36) Kasha, M.; Rawls, H. R.; Ashraf El-Bayoumi, M. The exciton model in molecular spectroscopy. *Pure Appl. Chem.* **1965**, *11*, 371−392.
(37) Parkash, J.; Robblee, J. H.; Agnew, J.; Gibbs, E.; Collings, P.; Pasternack, R. F.; de Paula, J. C. Depolarized resonance light scattering by porphyrin and chlorophyll a aggregates. *Biophys. J.* **1998**, *74*, 2089−2099.
(38) Desiraju, G. R. C-H···O and other weak hydrogen bonds. From crystal engineering to virtual screening. *Chem. Commun.* **2005**, *24*, 2995−3001.
(39) Desiraju, G. R.; Steiner, T. *The Weak Hydrogen Bond in Structural Chemistry and Biology*; Oxford University Press: Oxford, U.K., 2001.
(40) Mazerski, J.; Borowski, E. Molecular dynamics of amphotericin B. II. Dimer in water. *Biophys. Chem.* **1996**, *57*, 205−217.
(41) Gruszecki, W. I. Carotenoids in Membranes. In *The Photochemistry of Carotenoids*; Frank, H. A., Young, A. J., Britton, G., Cogdell, R. J., Eds.; Kluwer Academic Publishers: Dordrecht, The Netherlands, 1999; Vol. *8*; pp 363−379.
(42) Gruszecki, W. I.; Smal, A.; Szymczuk, D. The effect of zeaxanthin on the thickness of dimyristoylphosphatidylcholine bilayer: X-ray diffraction study. *J. Biol. Phys.* **1992**, *18*, 271−280.
(43) Kühlbrandt, W.; Wang, D. N. Three-dimensional structure of plant light-harvesting complex determined by electron crystalography. *Nature* **1991**, *350*, 130−134.
(44) Gruszecki, W. I.; Gagos, M.; Herec, M.; Kernen, P. Organization of antibiotic amphotericin B in model lipid membranes. A mini review. *Cell. Mol. Biol. Lett.* **2003**, *8*, 161−170.
(45) De Kruijff, B.; Demel, R. A. Polyene antibiotic−sterol interaction in membranes of Acholeplasma Laidlawii cells and lecithin liposomes; III. Molecular structure of the polyene antibiotic-cholesterol complex. *Biochim. Biophys. Acta* **1974**, *339*, 57−70.